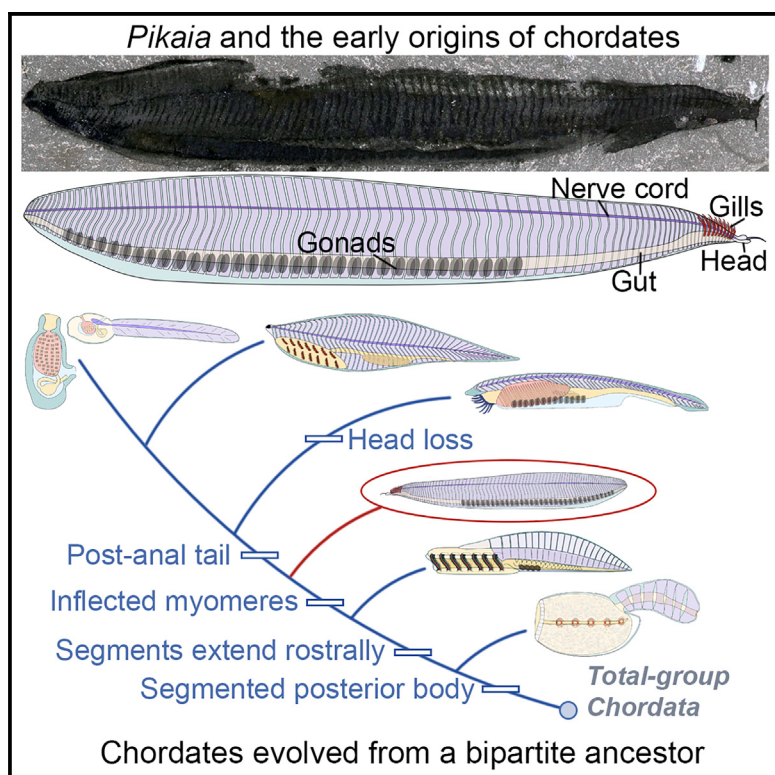


## A new interpretation of *Pikaia* reveals the origins of the chordate body plan

### Graphical abstract



### Authors

Giovanni Mussini, M. Paul Smith,  
Jakob Vinther, Imran A. Rahman,  
Duncan J.E. Murdock,  
David A.T. Harper, Frances S. Dunn

### Correspondence

gm726@cam.ac.uk

### In brief

Mussini et al. identify a gut canal and a dorsal nerve chord in the Cambrian fossil *Pikaia* and resolve it as a stem-group chordate. Their morphological reinterpretation of *Pikaia* establishes phylogenetic links between vertebrates, amphioxus, and problematic Cambrian fossils with a bipartite body plan, unveiling a cryptic chapter in chordate history.

### Highlights

- We describe a dorsal nerve cord and a gut canal in the Cambrian fossil *Pikaia*
- Its character combination identifies *Pikaia* as an unambiguous stem-group chordate
- *Pikaia*, *Yunnanozoon*, and vetulicolians record a chordate stem lineage
- Cambrian fossils support Romer's "somatico-visceral" hypothesis of chordate origins

## Report

# A new interpretation of *Pikaia* reveals the origins of the chordate body plan

Giovanni Mussini,<sup>1,7,\*</sup> M. Paul Smith,<sup>2</sup> Jakob Vinther,<sup>3,4</sup> Imran A. Rahman,<sup>2,5</sup> Duncan J.E. Murdock,<sup>2</sup> David A.T. Harper,<sup>6</sup> and Frances S. Dunn<sup>2</sup>

<sup>1</sup>University of Cambridge, Department of Earth Sciences, Downing Street, Cambridge CB2 3EQ, UK

<sup>2</sup>Oxford University Museum of Natural History, Parks Road, Oxford OX1 3PW, UK

<sup>3</sup>University of Bristol, School of Earth Sciences, Wills Memorial Building, Bristol BS8 1RL, UK

<sup>4</sup>University of Bristol, School of Biological Sciences, 24 Tyndall Avenue, Bristol BS8 1TQ, UK

<sup>5</sup>The Natural History Museum, Cromwell Road, South Kensington, London SW7 5BD, UK

<sup>6</sup>Durham University, Department of Earth Sciences, Lower Mountjoy, Durham DH1 3LE, UK

<sup>7</sup>Lead contact

\*Correspondence: gm726@cam.ac.uk

<https://doi.org/10.1016/j.cub.2024.05.026>

## SUMMARY

Our understanding of the evolutionary origin of Chordata, one of the most disparate and ecologically significant animal phyla, is hindered by a lack of unambiguous stem-group relatives. Problematic Cambrian fossils that have been considered as candidate chordates include vetulicolians,<sup>1</sup> *Yunnanozoon*,<sup>2</sup> and the iconic *Pikaia*.<sup>3</sup> However, their phylogenetic placement has remained poorly constrained, impeding reconstructions of character evolution along the chordate stem lineage. Here we reinterpret the morphology of *Pikaia*, providing evidence for a gut canal and, crucially, a dorsal nerve cord—a robust chordate synapomorphy. The identification of these structures underpins a new anatomical model of *Pikaia* that shows that this fossil was previously interpreted upside down. We reveal a myomere configuration intermediate between amphioxus and vertebrates and establish morphological links between *Yunnanozoon*, *Pikaia*, and uncontroversial chordates. In this light, we perform a new phylogenetic analysis, using a revised, comprehensive deuterostome dataset, and establish a chordate stem lineage. We resolve vetulicolians as a paraphyletic group comprising the earliest diverging stem chordates, subtending a grade of more derived stem-group chordates comprising *Yunnanozoon* and *Pikaia*. Our phylogenetic results reveal the stepwise acquisition of characters diagnostic of the chordate crown group. In addition, they chart a phase in early chordate evolution defined by the gradual integration of the pharyngeal region with a segmented axial musculature, supporting classical evolutionary-developmental hypotheses of chordate origins<sup>4</sup> and revealing a “lost chapter” in the history of the phylum.

## RESULTS

*Pikaia gracilens* Walcott, 1911<sup>5</sup> from the Burgess Shale of British Columbia (Wulian Stage, Miao Lingian Series, c. 508 Ma) represents the first potential Cambrian chordate to be recognized.<sup>2,3,6</sup> Nonetheless, the established model of *Pikaia*'s anatomy<sup>3</sup> shows conspicuous discrepancies with living chordates<sup>3,7,8</sup>: no clearly preserved dorsal nerve cord; no evident ventral digestive tract posterior to the foregut, despite the latter's recurrent preservation among 114 described specimens<sup>3,7</sup>; an internal, cuticularized, rod-like “dorsal organ”<sup>3,7,8</sup>; a continuous “ventral blood vessel” unlike the branched main ventral vessels of amphioxus and vertebrates<sup>7</sup>; ventrally oriented “anterior appendages” lacking counterparts among chordate gills<sup>3</sup>; and myomere boundaries with apices pointing in the direction opposite those of amphioxus and vertebrates.<sup>3,7,8</sup> Given these discrepancies and a lack of unambiguous chordate synapomorphies, several authors have suggested alternative placements among protostomes.<sup>9–11</sup>

We reinterpret *Pikaia*'s morphology following the recognition of the ventral blood vessel<sup>3</sup> as a nerve cord and of the dorsal

organ<sup>3</sup> as a gut, justified below. This supports a dorsoventrally inverted *Pikaia* relative to the traditional interpretation, given that by comparison with all known bilaterians<sup>12</sup> the gut canal of *Pikaia* could not have run along the dorsal margin of the body.

### Digestive tract

In their detailed study of *Pikaia*, Conway Morris and Caron<sup>3</sup> identified a longitudinal tube-like structure running alongside one of the body edges, which they labeled a dorsal organ acting as an internalized support or storage structure.<sup>3</sup> However, the dorsal organ has proved difficult to reconcile with the anatomy of any living or fossil groups.<sup>3,7,8</sup>

Our reinterpretation of the dorsal organ as a digestive tract, speculatively suggested in Lacalli,<sup>8</sup> is justified by the observation that the organ broadens and extends into the previously identified pharyngeal region<sup>3</sup> (Figures 1E, 1F, 1J–1L, 2F, and 2J). Like the pharynx, parts of the organ are conspicuously three-dimensional<sup>3</sup> (Figures 1E, 1F, 1H, and 1L) and characterized by calcium phosphate mineralization,<sup>3</sup> revealed by energy-dispersive X-ray spectroscopy<sup>3</sup> (Figure 3 in Conway Morris and Caron<sup>3</sup>). As with other

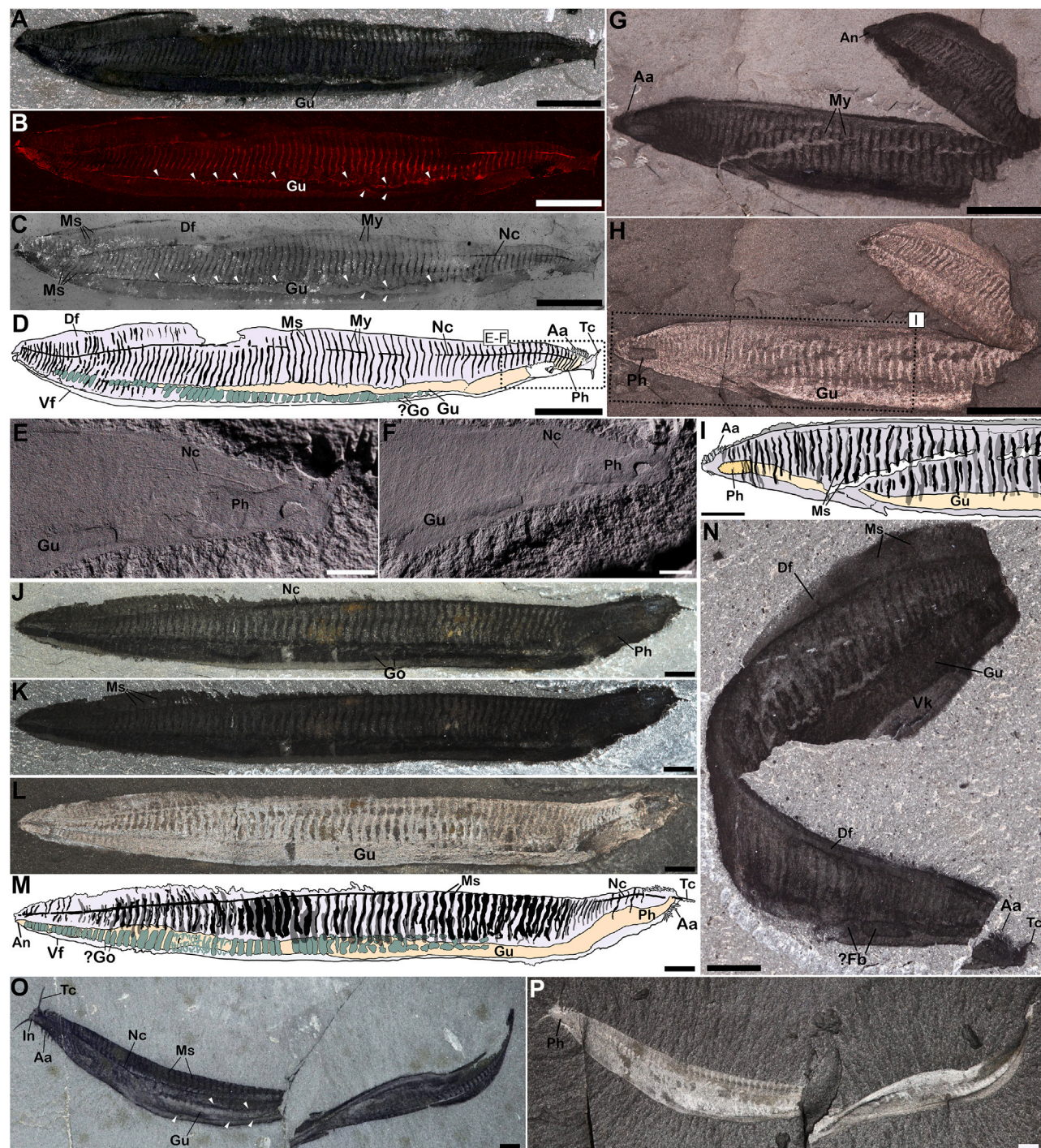


**Figure 1. Anatomical reinterpretation of *Pikaia gracilens* Walcott, 1911: General body plan, axial musculature, and digestive tract**

(A) USNM 198684, showing ventral gut canal, myosepta, and dorsal nerve cord. Note light-colored sediment infill of the gut canal, comparable to background matrix.

(B) Element map of (A) for carbon (C) obtained under energy-dispersive X-ray spectroscopy. Note dark, carbon-poor region of the gut canal, mapping onto the sediment infill in (A).

(C) View of (A) under backscattered scanning electron microscopy. Note light-colored sediment infill of the gut canal, comparable to background matrix.

(D) Interpretative drawing of (A)–(C).

(E) and (F) Photographs of regions corresponding to boxed area in (D) (part and counterpart), taken with specimen coated in ammonium chloride sublimate to highlight relief.

(G) USNM 198686.

(legend continued on next page)

# Current Biology Report



Burgess Shale-type macrofossils, this three-dimensionality implies resistance to compaction, either through original biomineralization (inconsistent with the organ's trajectory and morphology<sup>3</sup>) or diagenetic permineralization.<sup>3,13,14</sup> In Burgess Shale-type deposits, early diagenetic permineralization denotes labile, chemically reactive tissues, particularly gut and cecal systems.<sup>13,14</sup> Additionally, anterior tracts of the organ are preserved with light-colored sediment infills (cf. Hughes<sup>15</sup>) similar to the surrounding matrix (Figures 1A–1C and 1O), suggesting that it was externally open rostrally. Overall, the organ's reflectivity, color, morphology, and relief<sup>3</sup> match those of unambiguous gut tissues from other Burgess Shale-type macrofossils, including the chordate *Metaspriggina* (cf. Conway Morris and Caron<sup>16</sup>; Figures 1 and S1; cf. Butterfield, Hughes, and Briggs and Whittington<sup>13–15,17</sup>).

*Pikaia*'s newly identified digestive tract is delineated by diffuse carbonaceous margins (Figures 1A–1C, 1O, 2A, 2F, 2I, and 2J), also visible in *Metaspriggina*<sup>16</sup> (Figure 1; Figure S5 in Conway Morris and Caron<sup>16</sup>) and consistent with a pigmented or lipid-rich peritoneum (cf., e.g., Heingård et al.<sup>20</sup>). Previously uncharacterized, internal lensoid structures suggestive of food boluses (cf., e.g., Tian et al.<sup>21</sup>; Figures 1N<sup>3</sup> and 2; Figure 12A in Conway Morris and Caron<sup>3</sup>) also support a digestive function. Furthermore, some specimens preserve repeated, organic-rich rounded structures with indistinct outlines, flanking the gut ventrally (Figures 1A–1D, 1J–1M, S1F, and S1G) and morphologically similar to the female gonads of cephalochordates (e.g., Yamaguchi and Henmi<sup>22</sup>), *Mylokunmingia*,<sup>23</sup> and *Yunnanozoon*.<sup>18,24</sup> The modest positive relief of these structures relative to the gut canal (Figure 1L) explains its apparently wrinkled or "creased"<sup>3</sup> surface, previously interpreted as evidence for a cuticular wall.<sup>3</sup>

In summary, *Pikaia*'s digestive tract is identified by sediment infills, internal features interpreted as food boluses and phosphatized inclusions,<sup>3</sup> and carbonaceous margins. The digestive tract comprises an expanded anterior pharynx and a tubular gut varying in width but tapering caudally. The pharynx comprises ~7%–10% of the total body length and constricts into the tubular gut slightly posterior to *Pikaia*'s anterior appendages<sup>3</sup> (Figures 1A, 1E, 1F, 2H, and 2J). The digestive tract terminates at the body's caudal tip, indicating the absence of a post-anal tail (cf. Conway Morris and Caron<sup>16</sup>; Figures 1J–1M, 2I, and S1D).

## Nervous system

The dark longitudinal strand running along *Pikaia*'s traditionally interpreted ventral margin was tentatively described as a ventral blood vessel,<sup>3</sup> but this has been challenged<sup>7,25</sup> due to

its morphological differences with the main ventral vessels of amphioxus and vertebrates, which branch into a subenteric hepatic portal vein and a ventral aorta separated by hepatic capillaries.<sup>8</sup> The ventral blood vessel also lacks the adjoining vessels required to complete a circuit.<sup>25</sup> Accordingly, Conway Morris and Caron<sup>3</sup> hypothetically suggested that the "vessel" may have been a nerve cord. We support and extend this hypothesis by reinterpreting this structure, using new observations and recent advances in the taphonomy of nervous systems,<sup>26–28</sup> as a dorsal nerve cord (Figures 1A–1F, 1J–1M, 1O, 1P, 2A, S1A, S1C, and S1E).

The nerve cord is preserved as a highly organic-rich residue, consistent with nervous tissues from Burgess Shale-type localities.<sup>26–28</sup> Occasionally, it is fragmented, indicating that it behaved as a relatively brittle structure during decay and early diagenesis (Figures 2A, 2B, and S1A). It shows modest three-dimensional preservation (Figures 1E and 1F), in contrast to putative cardiovascular systems in Cambrian organically preserved fossils<sup>29</sup> (Figure 3A; cf. Figure 3B): its thickness is reflected by occasional uneven splitting between part and counterpart, leaving an intermittent groove in place of original nerve cord tracts (cf. Ortega-Hernández et al.<sup>26</sup> and Figure 1) (e.g., Figure 2H; cf. Figure 3H). The nerve cord thickens rostrally into a "bulb"-like<sup>3</sup> region (Figures 2B, 2C, and S1E), reminiscent of the tubular brain of cephalochordates and embryonic vertebrates,<sup>30</sup> before bifurcating into two carbonaceous strands extending into the innervations<sup>3</sup> of *Pikaia*'s cephalic tentacles (Figures 2B, 2C, and 2H–2K; Figures 10B–10G, 10J, and 11A–11D in Conway Morris and Caron<sup>3</sup>). Together, the well-defined carbonaceous preservation, bilateral symmetry, and topology of *Pikaia*'s nervous system exclude alternative interpretations including cardiovascular or microbial origins<sup>26</sup> (cf. Liu et al.<sup>31</sup>).

We find no apparent notochord associated with the dorsal nerve cord in *Pikaia*, and no notochord was conclusively identified by previous studies<sup>3,7,8,25</sup> (Data S1, character 168). However, this may not reflect a genuine absence given the frequent lack of visible notochords in unambiguous crown-chordate fossils (e.g., Gabbott et al.<sup>32</sup>).

## Myomeres

As shown by Conway Morris and Caron,<sup>3</sup> the organic-rich transverse strands on the trunk of well-preserved *Pikaia* specimens are best interpreted as intercalary spaces between myomeres, coincident with the lipid-rich myosepta<sup>3</sup> (cf. Briggs and Kear and Sansom et al.<sup>33,34</sup>). This interpretation is supported by their

(H) Photograph of (G) coated in ammonium chloride sublimate, showing anterior pharynx in negative relief.

(I) Interpretative drawing of boxed area in (G) and (H); reflective myosepta are represented in dark gray; carbonaceous impressions of myosepta in black.

(J) ROMIP 61236, showing fully preserved digestive tract.

(K) (J) photographed under polarized light.

(L) (J) photographed with ammonium chloride sublimate coating to highlight relief of the gut canal.

(M) Interpretative drawing of (J)–(L); reflective myosepta are represented in dark gray; carbonaceous impressions of myosepta in black.

(N) ROMIP 951804, showing laterally compressed dorsal "fin"<sup>3</sup> in profile and frontal view and digestive tract with potential food boluses.

(O) USNM 57628 (lectotype), showing the caudal section of the trunk rotated and preserved in oblique view. Note light-colored sediment infill of the gut canal.

(P) Specimen in (O) photographed with ammonium chloride sublimate coating to highlight relief of gut canal.

USNM, Department of Paleobiology, National Museum of Natural History, Smithsonian Institution; ROMIP, Royal Ontario Museum, Invertebrate Palaeontology; Df, dorsal fin; Vf, ventral fin; Ms, myosepta; My, myomeres; Nc, dorsal nerve cord; Aa, anterior appendages; ?Go, possible gonads; Gu, gut canal; Ph, pharyngeal cavity; An, anus; Tc, tentacles; In, innervation. White arrows in (B), (C), and (O) denote carbonaceous margins associated with the gut canal. Scale bars, 5 mm (A–D, G, and H); 1 mm (E, F, and I); 2 mm (other panels).

See also Figure S1 and Data S1 and S2.

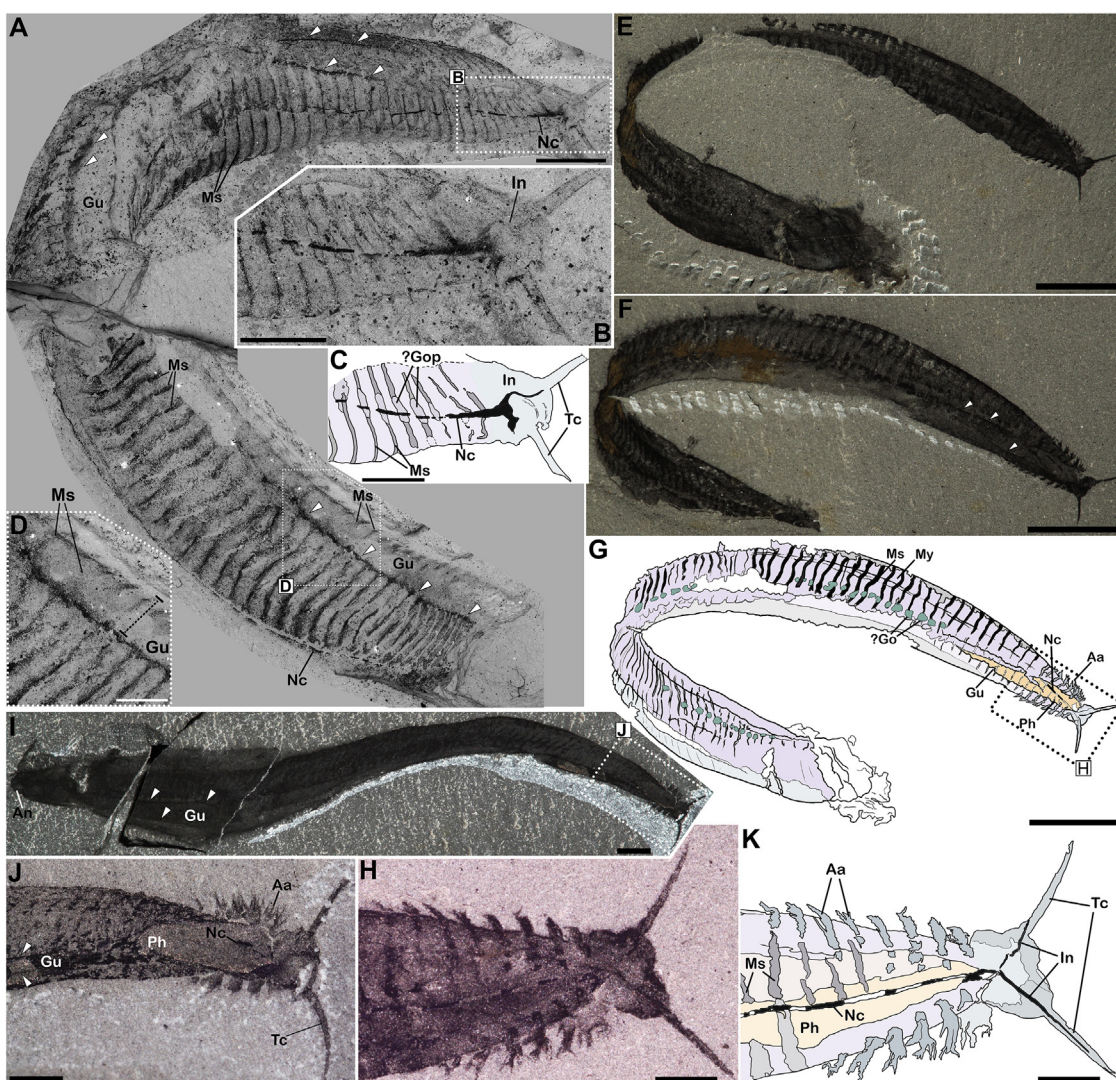


**Figure 2. Anatomical reinterpretation of *Pikaia gracilens* Walcott, 1911: Nervous system and axial musculature**

(A) Composite image of USNM 202220 under backscattered scanning electron microscopy, showing dark carbon-rich stains corresponding to the myosepta, nervous system remnants, and margins of the gut canal.

(B) Detail of boxed area in (A) showing thickened rostral portion of the dorsal nerve cord, partly preserved innervations of the tentacles, and apparent integumentary perforations recording possible gill openings.

(C) Interpretative drawing of (B).

(D) Detail of corresponding box in (A); dotted line denotes extension of myomeres spanning the width of the gut canal.

(E and F) USNM 198688 (part and counterpart).

(G) Interpretative drawing of USNM 198688 combining part and counterpart.

(H) Detail of boxed area in (F) highlighting rostral portion of the nerve cord, anterior appendages, and cephalic structures.

(I) ROMIP 951067.

(J) Detail of boxed area in (H) showing pharyngeal cavity, anterior-most midgut, and partly preserved nerve cord tract.

(K) Interpretative drawing of (G).

USNM, Department of Paleobiology, National Museum of Natural History, Smithsonian Institution; ROMIP, Royal Ontario Museum, Invertebrate Palaeontology; ?Gop, possible gill openings; Ms, myosepta; Nc, nerve cord; In, innervation; Tc, tentacle; My, myomeres; ?Go, possible gonads; Gu, gut canal; Ph, pharynx; An, anus; Aa, anterior appendages. Scale bars, 2 mm (A and I); 1 mm (B–D, H, J, and K); 5 mm (E–G). White arrows in (A), (F), (I), and (J) denote carbonaceous margins associated with the gut canal.

See also Figure S1 and Data S1, S2, and S3.

orderly arrangement and regular spacing (Figures 1A–1D, 1J, 1K, 2A, S1B, and S1F). Both contrast with the disorganized, offset configuration of similar organic-rich strands in decayed modern

chordates<sup>33,34</sup> and *Metaspriggina*,<sup>16</sup> which are often directly superimposed on the matrix following decomposition of surrounding tissues<sup>16</sup> (cf. Briggs and Kear<sup>33</sup>). This argues against

# Current Biology Report

CellPress  
OPEN ACCESS

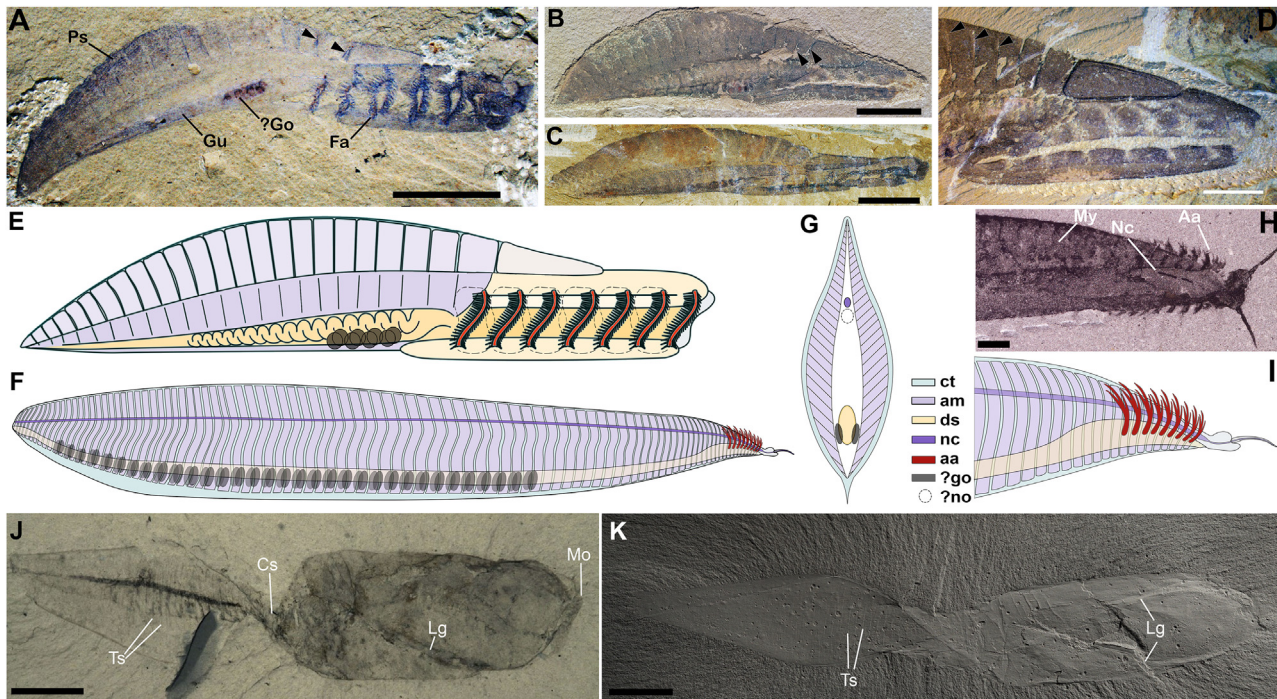


**Figure 3. Representative stem-group chordates and comparisons with *Pikaia***

(A–E) *Yunmanozoon*.

(A) RCCBYU 10310, showing gut tube, posterior segments, and filamentous arches.

(B) YKLP 13005.

(C) YKLP 13032.

(D) YKLP 13016. Black arrows denote separation between dorsal “segments.”

(E) Schematic anatomical reconstruction after Cong et al. and Tian et al.<sup>18,19</sup>

(F) *Pikaia*, schematic reconstruction illustrating dorsoventrally inverted anatomical reinterpretation.

(G) Hypothetical cross-sections of trunk segments in *Pikaia*<sup>3</sup> under the new dorsoventrally inverted interpretation, showing dorsal and ventral “fins.”<sup>3</sup> Color legend on the right applies to (E)–(I).

(H) USNM 198688, detail of the anterior region showing bilobed head, anterior appendages, pharyngeal cavity, and dorsal nerve cord.

(I) Schematic reconstruction of the anterior region of *Pikaia* under the new anatomical interpretation, showing the anterior appendages as dorsally directed gills.

(J and K) *Banffia constricta*.

(J) ROMIP 49914.

(K) ROMIP 49898, photographed under ammonium chloride sublimate to highlight relief of lateral grooves and segmental boundaries.

RCCBYU, Research Center of Chengjiang Biota, Yunnan University, Kunming; YKLP, Yunnan Key Laboratory for Palaeobiology, Kunming; USNM, Department of Paleobiology, National Museum of Natural History, Smithsonian Institution; ROMIP, Royal Ontario Museum, Invertebrate Palaeontology; Ps, posterior segments; Gu, gut; ?Go, possible gonads; Fa, filamentous arches; ct, connective tissue, integument; am, axial musculature; ds, digestive system; nc, dorsal nerve cord; aa, anterior appendages; ?no, hypothetical notochord; My, myomeres; Ph, pharynx; Lg, lateral grooves; Cs, constriction; Ts, tail segments; Mo, mouth opening. Scale bars, 5 mm (A, C, and D); 10 mm (B, J, and K); 1 mm (H).

See also Data S1 and S2.

interpreting *Pikaia*'s strands as decaying myomeres shrunk away from myosepta<sup>3,33</sup> and provides a counterpart to probable myosepta described in fossil vertebrates.<sup>33</sup>

Our reinterpretation establishes a new orientation for *Pikaia*'s myomeres (cf. Conway Morris and Caron<sup>3</sup>). The myomeres, defined by the spaces between the observed myosepta, are sigmoidal along their dorsoventral trajectory and kink or inflect anteriorly in the dorsal portion of the body (Figures 1A–1D, 1J–1M, S1B, S1F, and S1G), consistent with myomeres in crown chordates, including amphioxus, *Myllokunmingia*, and *Metaspriggina*.<sup>16,35,36</sup> Additionally, they sometimes show weaker, rostrally convex ventral inflections (Figures 1J, 1K, and 2D). The myomeres extend along *Pikaia*'s entire trunk, from behind the bilobed “head”<sup>3</sup> to the tip of the tail. Caudally, myosepta

can be traced into the dorsal “fin”<sup>3</sup> as fainter impressions (Figures 1A–1C, 1J–1N, and S1H), consistent with them occupying a reduced volume within this laterally compressed extension of the trunk<sup>3</sup> (Figure 1N).

## External features—fins and gills

Conway Morris and Caron identified laterally compressed dorsal and ventral median “fins” in *Pikaia*,<sup>3</sup> inverted in our reconstruction. In the reoriented configuration, a thin, keel-like ventral fin extends for about 80% of the total body length, whereas a more prominent posterior dorsal “fin”<sup>3</sup> extends for 30%–40% of total body length. Both fins terminate at the caudal tip of the body. Unlike in crown chordates, the myomeres extend into the dorsal “fin”<sup>3</sup> (Figures 1A–1D, 1J–1N, and S1H) with no

evidence for supportive fin rays, suggesting that the fin was more robust and less clearly demarcated from the trunk than in extant chordates.

*Pikaia*'s external, filamentous "anterior appendages"<sup>3</sup> (Figures 2H, 2J, 2K, 3H, and 3I) match the configuration of free-hanging gills in aquatic vertebrates and bilaterians more generally, oriented dorsally and away from the substrate (e.g., Nokhbatolfoghahai and Downie and Stundl et al.<sup>37,38</sup>). Their branching morphology and similar preservation of these structures as organic-rich stains in both vertebrate and invertebrate fossils (cf. Gao and Shubin and Caron et al.<sup>39,40</sup>) further support an interpretation as gills.<sup>3</sup>

### Phylogenetic analysis

Our novel interpretation of *Pikaia* informed a new deuterostome-focused phylogenetic analysis, including 102 taxa and 625 characters (Data S2) and sampling extensively from Li et al. and Tian et al.<sup>41,19</sup> (Data S1). Twenty-five new characters in our analyses (Data S1) were subject to different scoring criteria testing the robustness of our topology to alternative anatomical interpretations (Data S2 and S3). We incorporated a number of other relevant fossil taxa exhibiting potential shared features with living chordates, including vetulicolians, *Yunnanozoon*, and the stem-group vertebrates *Metaspriggina*<sup>16</sup> and *Myllokunmingia*<sup>23,35</sup> (Data S2 and S3).

Vetulicolians (Figures 3J and 3K) and *Yunnanozoon* (Figures 3A–3D) show a bipartite body plan with an "anterior body" occupied by a pharynx lined by lateral arches or pores and a "posterior body" partitioned into metamerized units with a recalcitrant body wall.<sup>18,19,42,43–46</sup> Both taxa lack apparent myomeres or myosepta,<sup>18,42,47,45,46</sup> which preserve consistently in other fossils from the same deposits.<sup>23,35</sup> The anterior body of both taxa comprises two sclerotized "halves" joined along the lateral sides to form a groove-like region, clearly opened to the exterior in vetulicolids<sup>43</sup> and lined by the pharyngeal openings.<sup>18,42–47</sup> The digestive tract extends through the caudal region: in vetulicolians, it extends medially and opens into a terminal anus; in *Yunnanozoon* it is displaced ventrally as in *Pikaia*.<sup>18,19,42,43–46</sup>

Tree searches were performed in MrBayes 3.2.7,<sup>48</sup> using Bayesian Inference under an MK + gamma model.<sup>49</sup> We recover *Pikaia* as a stem chordate, subtending the crown node with high posterior probability ( $p = 98$ ; Figure 4A). Together with *Yunnanozoon* and *Cathaymyrus*,<sup>6</sup> *Pikaia* forms a grade of stem chordates crownward of vetulicolians, resolved as a grade of earlier diverging chordates (Figure 4A). The topology is robust to alternative character coding, taxon sampling, and model choices (Data S1; Figures S2–S4). The alternative scenario of vetulicolian monophyly is recovered as unlikely in our steppingstone sampling analysis ( $2 \times \log_e B_{10} = -7.20$ ; Table S1).

### DISCUSSION

Our reinterpretation of *Pikaia* provides new evidence for diagnostic chordate synapomorphies: a dorsal nerve cord and unambiguous myomeres.<sup>3,51</sup> By contrast, *Pikaia*'s digestive tract has a terminal anus, unlike in crown chordates,<sup>16,35,41</sup> which possess a post-anal tail.<sup>16,35,41</sup> We resolve *Pikaia* as a stem chordate (Figures 4 and S2–S4), elucidating the sequence of character acquisition in the group.

The sigmoidal myosepta of *Pikaia*<sup>3</sup> show conspicuous dorsal inflections pointing cranially, as in vertebrates<sup>7,16,35</sup> and amphioxus,<sup>7,25,35</sup> but their weakly recurved ventral sections confirm a more similar shape to vertebrates.<sup>7</sup> *Pikaia*'s weakly bent myomeres are intermediate between the steeply angled crown-chordate muscle blocks<sup>7,16,25,35,36</sup> and the subrectangular axial units of *Yunnanozoon*,<sup>18,42,43,47,52</sup> recovered immediately stemward of *Pikaia* (Figures 4A and 4C). This topology suggests a transition toward increasingly inflected segmental musculature along the chordate stem<sup>25</sup> (Figure 4C), likely accompanying the evolution of faster, more powerful swimming.<sup>25</sup> The anatomical correspondence between myomeres and yunnanozoan axial units is independently supported by the extension of myomeres into *Pikaia*'s dorsal fin. Metameric muscle blocks extending into a dorsal fin<sup>3</sup> are unknown in crown chordates<sup>7,16,25,35,36</sup> but find plausible counterparts in *Yunnanozoon*'s fin-like dorsal region,<sup>18,42,43,47</sup> partitioned into segmental blocks (Figures 3A–3E). Therefore, homology between myomeres and *Yunnanozoon*'s axial units is upheld by positional and morphological similarity, as well as congruence with other homologies<sup>53</sup>: *Pikaia*'s filamentous "anterior appendages,"<sup>3</sup> suggestive of external free-hanging gills, further support an affinity with *Yunnanozoon* by providing a counterpart to its similarly exposed and filamentous arches<sup>3,19</sup> (Figures 3A and 3E<sup>18,42,43,47</sup>).

*Yunnanozoon*, in turn, shares characters with the vetulicolians, recovered as stem-group chordates.<sup>41,19,52</sup> These include a bipartite body plan with a voluminous anterior pharynx and a segmented tail, a medial anterior cleft reminiscent of the vetulicolian "lateral groove," and a robust cuticle-like integument<sup>18,42–47,52,54</sup> (Figures 3A–3E). The homology of these characters is supported by our phylogenetic results (Figures 4A and S2–S4). A chordate placement for vetulicolians<sup>41,19,52</sup> fits with the recognition of a terminal anus in stem-group ambulacrarians,<sup>41</sup> supporting independent origins of post-anal structures in ambulacrarians and chordates<sup>41</sup> and undermining the main rationale for an alternative, stem-deuterostome placement.<sup>46</sup> Serialized lateral openings, segments of probable mesodermal<sup>45</sup> origin, a voluminous anterior pharynx, and laterally compressed bodies in most vetulicolians also support a chordate affinity.<sup>1,41</sup> However, unlike other vetulicolians, banffozoans (Figures 3J and 3K)—recovered for the first time as the earliest diverging stem chordates (Figure 4A)—lack a laterally compressed body plan and visible lateral pouches or other serialized pharyngeal structures,<sup>44,46,54</sup> suggesting that these traits were acquired in a stepwise fashion in a paraphyletic vetulicolian stem group (Figure 4A). If so, pharyngeal openings in the deuterostome last common ancestor might have been non-serialized pores,<sup>41,55</sup> as in the stem-group ambulacrarian *Herpetogaster*.<sup>41,50</sup>

The grade of "bipartite animals" comprising vetulicolians and *Yunnanozoon* on the chordate stem prompts us to propose a new evolutionary scenario reminiscent of Romer's "somatico-visceral" hypothesis of chordate origins<sup>4</sup> (Figure 4B). Drawing on vertebrate neuroanatomy and metamericism, and inspired by Garstang's<sup>56</sup> tunicate-based model of the chordate ancestor, Romer proposed that the archetypal chordate bauplan was subdivided into a "somatic"<sup>4</sup> posterior body comprising the central nervous system, axial skeleton, and somites and a "visceral"<sup>4</sup> anterior, encompassing the pharynx and digestive organs. Romer's hypothesis addressed the distinct embryonic origins and

# Current Biology Report

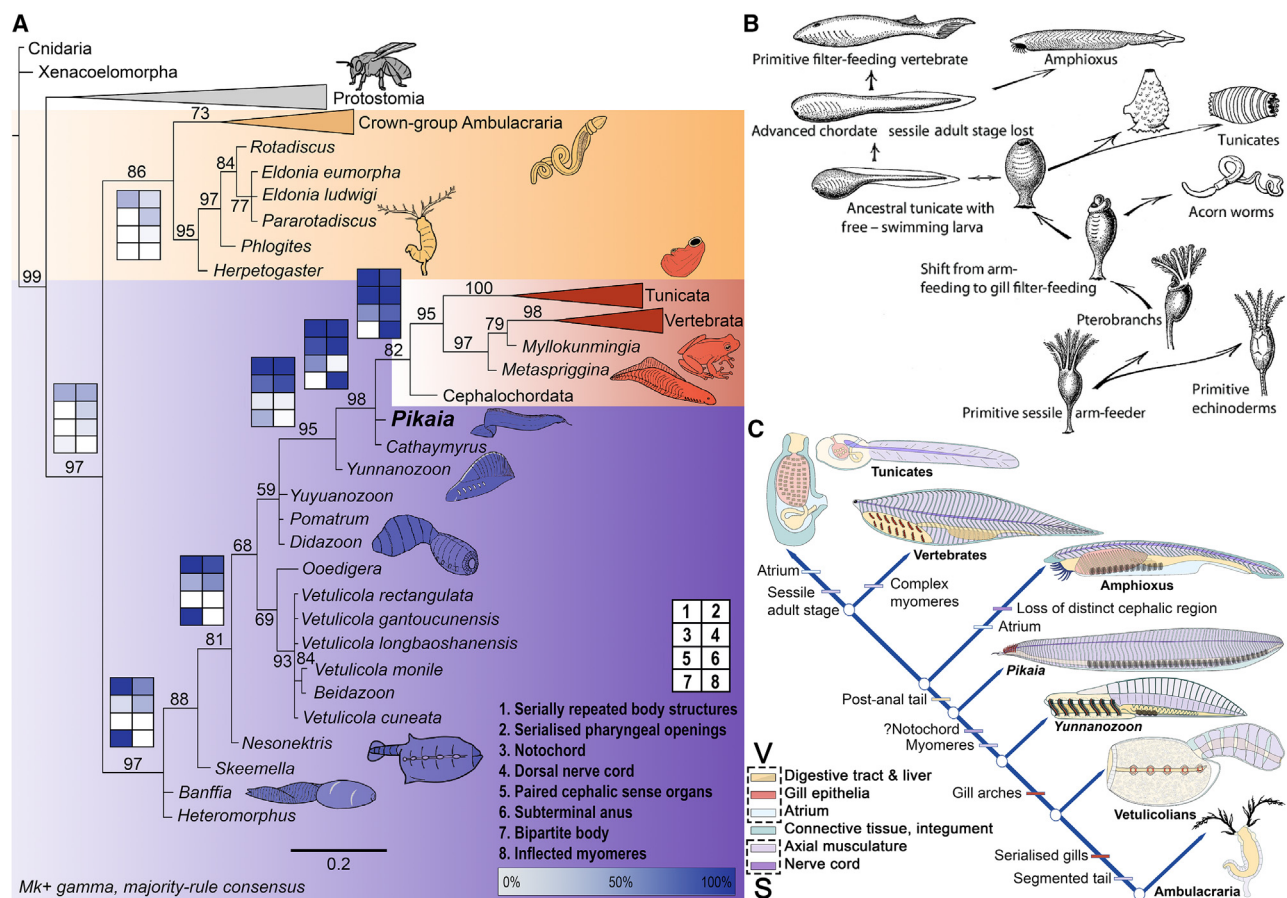


**Figure 4. The phylogenetic relationships and evolutionary implications of stem-group chordates**

(A) Phylogenetic tree of Bilateria based on Bayesian inference (BI), showing the position of *Pikaia* and other Cambrian deuterostomes. Branch lengths are proportional to the number of character state changes (scale bar on the bottom left). Node numbers indicate posterior probability values (BI). Tie plots show reconstructed ancestral state probabilities (0% to 100%; legend on the bottom right) at their corresponding nodes. Yellow background shading denotes ambulacrarians; purple, stem-group chordates; red, crown-group chordates.

(B) Romer's hypothetical "somatico-visceral" scenario of chordate evolution, adapted from Romer,<sup>4</sup> for comparison with our updated hypothesis in (C).

(C) Scenario of chordate evolution based on (A), charting the integration of somatic<sup>4</sup> (S) and visceral<sup>4</sup> (V) components (legend at the bottom left) and the acquisition of key chordate characters (colored bars). Stem-group vertebrate (*Metaspiggina*) after Morris and Caron,<sup>16</sup> *Yunnanozoon* after Cong et al. and Tian et al.,<sup>18,19</sup> and stem-group ambulacrarian (*Herpetogaster*) after Caron et al.<sup>50</sup>

See also Data S1, S2, and S3 and Figures S2–S4.

anatomical offset of chordate somites and gill arches and their manifestations in associated muscular, nervous, and skeletal structures.<sup>4</sup> It envisaged a gradual integration of the two "bodies," with the "visceral" encapsulated by the anterodorsal extension of the "somatic."<sup>4</sup>

Gee<sup>1</sup> speculated that the bipartite vetulicolian body plan embodied Romer's<sup>4</sup> hypothetical ancestral chordate. Under this interpretation, the "somatic" posterior unit would correspond to the segmented tail of vetulicolians, and the "visceral" unit to the anterior body.<sup>1</sup> This hypothesis is supported by recovering a grade of vetulicolians stemward of all other chordates and reconstructing their bipartite condition as plesiomorphic for the phylum (Figures 4A and S2–S4). Moreover, the recovery of *Yunnanozoon* as a phylogenetic intermediate between vetulicolians and more derived chordates lacking a bipartite body plan (Figure 4C) supports a trend toward greater integration of the two "bodies"<sup>4</sup> along the chordate stem.

Our revised "somatico-visceral"<sup>4</sup> model fits evolutionary-developmental data revealing highly conserved gene-regulatory elements among deuterostomes, including modular gene clusters underpinning gill-slit development,<sup>57</sup> cardiopharyngeal regulatory networks,<sup>58</sup> and core modules for notochord and neural tube development.<sup>59</sup> These discrete gene-regulatory elements, showing conserved and functionally important syntenic linkages,<sup>57</sup> suggest ancient origins as distinct developmental and functional modules for the defining "visceral" and "somatic" organs<sup>4</sup>: the pharyngeal apparatus,<sup>57</sup> and the central nervous system and axial skeleton.<sup>59</sup> Moreover, our hypothesis reconciles stem-chordate morphologies with the conserved organization and Hox gene expression patterns of the deuterostome trunk (cf. Lacalli<sup>8</sup>): the vetulicolian and *yunnanozoon* "posterior bodies" would comprise somite homologs, whereas the gill-bearing anterior would embody the condition of the trunk prior to the evolution and rostral extension of somites,<sup>1,4</sup>

as exemplified by hemichordates<sup>8</sup> and possibly early-diverging echinoderms.<sup>60</sup> By contrast, both the bilobed cephalic unit of *Pikaia* and the lobate circumoral rim of *Yunnanozoon*<sup>3,19</sup> lie anterior to the trunk and therefore the anterior-most boundary of Hox gene expression,<sup>8</sup> supporting a “head” identity. *Pikaia*’s distinct head with paired, cerebrally innervated sense organs suggests simplification of the anterior central nervous system in amphioxus (Figures 4A and S2B), consistent with secondary losses of complex neuroectodermal signaling centers in cephalochordates.<sup>61</sup>

This scenario restores *Pikaia* from specialized and phylogenetically “peripheral”<sup>7,35</sup> to a keystone evolutionary intermediate, illuminating the morphology of the chordate LCA (Figure 4). *Pikaia* and other Cambrian problematica exhibit a mosaic of overlapping plesiomorphic features and nested subsets of crown-group traits, as expected for stem-group relatives of any clade.<sup>62</sup> Our scenario also restores Romer’s “dual animal”<sup>14</sup> from useful heuristic device<sup>63</sup> to genuine evolutionary model, supplying a historical explanation for the evolutionary-developmental evidence in its favor<sup>1,57–59,64</sup> and elucidating the assembly of an ecologically revolutionary body plan.<sup>65,66</sup>

## STAR★METHODS

Detailed methods are provided in the online version of this paper and include the following:

- KEY RESOURCES TABLE
- RESOURCE AVAILABILITY
  - Lead contact
  - Materials availability
  - Data and code availability
- EXPERIMENTAL MODEL AND SUBJECT DETAILS
- METHOD DETAILS

## SUPPLEMENTAL INFORMATION

Supplemental information can be found online at <https://doi.org/10.1016/j.cub.2024.05.026>.

## ACKNOWLEDGMENTS

We are grateful to Jean-Bernard Caron, the Royal Ontario Museum, and Peiyun Cong (Yunnan Key Laboratory for Palaeobiology) for providing the specimen photographs, backscatter images, and elemental maps used in Figures 1, 2, and 4. We thank Simon Conway Morris for useful discussion on an early draft of this manuscript, Degan Shu (Northwestern University) for sharing accession numbers of *Myllorukkingia* specimens used to code our Data S3 matrix, three anonymous referees for their constructive comments on an early version of this manuscript, and the Oxford Department of Zoology for project funding. F.S.D. acknowledges support from the Royal Commission for the Exhibition of 1851 and an NERC independent research fellowship (NE/W00786X/1). G.M. acknowledges support from an NERC C-CLEAR DTP studentship (RG96579). D.A.T.H. thanks the Leverhulme Trust (UK) for support.

## AUTHOR CONTRIBUTIONS

J.V. first suggested a dorsoventrally inverted reinterpretation of *Pikaia*. G.M., F.S.D., M.P.S., and J.V. conceptualized the study. G.M. conducted specimen descriptions and interpretations with input from J.V., F.S.D., and M.P.S.; G.M., F.S.D., M.P.S., I.A.R., J.V., and D.J.E.M. contributed to assembling the phylogenetic dataset. G.M. ran the phylogenetic analyses, made the figures, and wrote the original draft of the manuscript. All authors contributed to review and editing.

## DECLARATION OF INTERESTS

The authors declare no competing interests.

Received: March 7, 2024

Revised: April 19, 2024

Accepted: May 14, 2024

Published: June 11, 2024

## REFERENCES

1. Gee, H. (2001). On being vetulicolian. *Nature* 414, 407–409.
2. Chen, J.Y., Dzik, J., Edgecombe, G.D., Ramsköld, L., and Zhou, G.Q. (1995). A possible Early Cambrian chordate. *Nature* 377, 720–722.
3. Conway Morris, S., and Caron, J.B. (2012). *Pikaia gracilens* Walcott, a stem-group chordate from the Middle Cambrian of British Columbia. *Biol. Rev.* 87, 480–512.
4. Romer, A.S. (1972). The vertebrate as a dual animal—somatic and visceral. In *Evolutionary Biology* (Springer), pp. 121–156.
5. Walcott, C.D. (1911). Middle Cambrian annelids. *Smithsonian Misc. Collect.* 57, 109–144.
6. Shu, D.G., Conway Morris, S., and Zhang, X.L. (1996). A *Pikaia*-like chordate from the Lower Cambrian of China. *Nature* 384, 157–158.
7. Mallatt, J., and Holland, N. (2013). *Pikaia gracilens* Walcott: stem chordate, or already specialized in the Cambrian? *J. Exp. Zool. B Mol. Dev. Evol.* 320, 247–271.
8. Lacalli, T. (2024). The Cambrian fossil *Pikaia*, and the origin of chordate somites. *EvoDevo* 15, 1. <https://doi.org/10.1186/s13227-024-00222-6>.
9. Dzik, J. (2004). Anatomy and relationships of the Early Cambrian worm *Myoscolex*. *Zool. Scripta* 33, 57–69.
10. Sansom, R.S., Gabbott, S.E., and Purnell, M.A. (2010). Non-random decay of chordate characters causes bias in fossil interpretation. *Nature* 463, 797–800.
11. Janvier, P. (2015). Facts and fancies about early fossil chordates and vertebrates. *Nature* 520, 483–489.
12. Nielsen, C., Brunet, T., and Arendt, D. (2018). Evolution of the bilaterian mouth and anus. *Nat. Ecol. Evol.* 2, 1358–1376.
13. Butterfield, N.J. (2002). *Leanchoilia* guts and the interpretation of three-dimensional structures in Burgess Shale-type fossils. *Paleobiology* 28, 155–171.
14. Butterfield, N.J. (1990). Organic preservation of non-mineralizing organisms and the taphonomy of the Burgess Shale. *Paleobiology* 16, 272–286.
15. Hughes, C.P. (1975). Redescription of *Burgessia bella* from the Middle Cambrian Burgess Shale, British Columbia. *Fossils Strata* 4, 415–435.
16. Conway Morris, S., and Caron, J.B. (2014). A primitive fish from the Cambrian of North America. *Nature* 512, 419–422.
17. Briggs, D.E.G., and Whittington, H.B. (1985). Modes of life of arthropods from the Burgess Shale, British Columbia. *Trans. Roy. Soc. Edinb.* 76, 149–160.
18. Cong, P.Y., Hou, X.G., Aldridge, R.J., Purnell, M.A., and Li, Y.Z. (2015). New data on the palaeobiology of the enigmatic yunnanozoans from the Chengjiang Biota, Lower Cambrian, China. *Palaeontology* 58, 45–70.
19. Tian, Q., Zhao, F., Zeng, H., Zhu, M., and Jiang, B. (2022). Ultrastructure reveals ancestral vertebrate pharyngeal skeleton in yunnanozoans. *Science* 377, 218–222.
20. Heingård, M., Sjövall, P., Sylvestersen, R.L., Schultz, B.P., and Lindgren, J. (2021). Crypsis in the pelagic realm: evidence from exceptionally preserved fossil fish larvae from the Eocene Stolleklin Clay of Denmark. *Palaeontology* 64, 805–815.
21. Tian, L., Jie, Y., Jin-Bo, H., and Xi-Guang, Z. (2015). The feeding behaviour of the Cambrian tubicolous priapulid *Selkirkia*. *Lethaia* 48, 125–132.

# Current Biology Report



22. Yamaguchi, T., and Henmi, Y. (2003). Biology of the amphioxus, *Branchiostoma belcheri* in the Ariake Sea, Japan II. *Zoolog. Sci.* 20, 907–918.
23. Xian-Guang, H., Aldridge, R.J., Siveter, D.J., Siveter, D.J., and Xiang-Hong, F. (2002). New evidence on the anatomy and phylogeny of the earliest vertebrates. *Proc. Biol. Sci.* 269, 1865–1869.
24. Dzik, J. (1995). *Yunnanozoon* and the ancestry of chordates. *Acta Palaeontol. Pol.* 40, 341–360.
25. Lacalli, T. (2012). The Middle Cambrian fossil *Pikaia* and the evolution of chordate swimming. *EvoDevo* 3, 12–16.
26. Ortega-Hernández, J., Lerosey-Aubrill, R., and Pates, S. (2019). Proclivity of nervous system preservation in Cambrian Burgess Shale-type deposits. *Proc. Biol. Sci.* 286, 20192370.
27. Edgecombe, G.D., Ma, X., and Strausfeld, N.J. (2015). Unlocking the early fossil record of the arthropod central nervous system. *Philos. Trans. R. Soc. Lond. B Biol. Sci.* 370, 20150038.
28. Park, T.Y.S., Kihm, J.H., Woo, J., Park, C., Lee, W.Y., Smith, M.P., Harper, D.A.T., Young, F., Nielsen, A.T., and Vinther, J. (2018). Brain and eyes of *Kerygmacheila* reveal protocerebral ancestry of the panarthropod head. *Nat. Commun.* 9, 1019.
29. Ma, X., Cong, P., Hou, X., Edgecombe, G.D., and Strausfeld, N.J. (2014). An exceptionally preserved arthropod cardiovascular system from the early Cambrian. *Nat. Commun.* 5, 3560.
30. Benito-Gutiérrez, E., Gattori, G., Stemmer, M., Rohr, S.D., Schuhmacher, L.N., Tang, J., Marconi, A., Jékely, G., and Arendt, D. (2021). The dorso-anterior brain of adult amphioxus shares similarities in expression profile and neuronal composition with the vertebrate telencephalon. *BMC Biol.* 19, 1–19.
31. Liu, J., Steiner, M., Dunlop, J.A., and Shu, D. (2018). Microbial decay analysis challenges interpretation of putative organ systems in Cambrian fuxianhuids. *Proc. Biol. Sci.* 285, 20180051.
32. Gabbott, S.E., Donoghue, P.C.J., Sansom, R.S., Vinther, J., Dolocan, A., and Purnell, M.A. (2016). Pigmented anatomy in Carboniferous cyclostomes and the evolution of the vertebrate eye. *Proc. Biol. Sci.* 283, 20161151.
33. Briggs, D.E., and Kear, A.J. (1993). Decay of *Branchiostoma*: implications for soft-tissue preservation in conodonts and other primitive chordates. *Lethaia* 26, 275–287.
34. Sansom, R.S., Gabbott, S.E., and Purnell, M.A. (2011). Decay of vertebrate characters in hagfish and lamprey (Cyclostomata) and the implications for the vertebrate fossil record. *Proc. Biol. Sci.* 278, 1150–1157.
35. Shu, D.G., Luo, H.L., Conway Morris, S., Zhang, X.L., Hu, S.X., Chen, L., Han, J., Zhu, M., Li, Y., and Chen, L.Z. (1999). Lower Cambrian vertebrates from south China. *Nature* 402, 42–46.
36. Flood, P.R. (1968). Structure of the segmental trunk muscle in amphioxus: With notes on the course and “endings” of the so-called ventral root fibres. *Z. Zellforsch. Mikrosk. Anat.* 84, 389–416.
37. Nokhbatolfoghai, M., and Downie, J.R. (2008). The external gills of anuran amphibians: comparative morphology and ultrastructure. *J. Morphol.* 269, 1197–1213.
38. Stundl, J., Pospisilova, A., Jandzik, D., Fabian, P., Dobiasova, B., Minarik, M., Metscher, B.D., Soukup, V., and Cerny, R. (2019). Bichir external gills arise via heterochronic shift that accelerates hyoid arch development. *eLife* 8, e43531.
39. Gao, K.Q., and Shubin, N.H. (2001). Late Jurassic salamanders from northern China. *Nature* 410, 574–577.
40. Caron, J.B., Scheltema, A., Schander, C., and Rudkin, D. (2006). A soft-bodied mollusc with radula from the Middle Cambrian Burgess Shale. *Nature* 442, 159–163.
41. Li, Y., Dunn, F.S., Murdock, D.J.E., Guo, J., Rahman, I.A., and Cong, P. (2023). Cambrian stem-group ambulacrarians and the nature of the ancestral deuterostome. *Curr. Biol.* 33, 2359–2366.e2.
42. Shu, D., Conway Morris, S., Zhang, Z.F., Liu, J.N., Han, J., Chen, L., Zhang, X.L., Yasui, K., and Li, Y. (2003). A new species of yunnanozoan with implications for deuterostome evolution. *Science* 299, 1380–1384.
43. Ou, Q., Conway Morris, S., Han, J., Zhang, Z., Liu, J., Chen, A., Zhang, X., and Shu, D. (2012). Evidence for gill slits and a pharynx in Cambrian vetulicolians: implications for the early evolution of deuterostomes. *BMC Biol.* 10, 81.
44. Aldridge, R.J., Xian-guang, H., Siveter, D.J., Siveter, D.J., and Gabbott, S.E. (2007). The systematics and phylogenetic relationships of vetulicolians. *Palaeontology* 50, 131–168.
45. Shu, D.G., Conway Morris, S., Han, J., Chen, L., Zhang, X.L., Zhang, Z.F., Liu, H.Q., Li, Y., and Liu, J.N. (2001). Primitive deuterostomes from the Chengjiang Lagerstätte (Lower Cambrian, China). *Nature* 414, 419–424.
46. Vinther, J., Smith, M.P., and Harper, D.A.T. (2011). Vetulicolians from the Lower Cambrian Sirius Passet Lagerstätte, North Greenland, and the polarity of morphological characters in basal deuterostomes. *Palaeontology* 54, 711–719.
47. Shu, D.G., Conway Morris, S., Zhang, Z.F., and Han, J. (2010). The earliest history of the deuterostomes: the importance of the Chengjiang Fossil Lagerstätte. *Proc. Biol. Sci.* 277, 165–174.
48. Ronquist, F., Teslenko, M., Van Der Mark, P., Ayres, D.L., Darling, A., Höhna, S., Larget, B., Liu, L., Suchard, M.A., and Huelsenbeck, J.P. (2012). MrBayes 3.2: efficient Bayesian phylogenetic inference and model choice across a large model space. *Syst. Biol.* 61, 539–542.
49. Lewis, P.O. (2001). A likelihood approach to estimating phylogeny from discrete morphological character data. *Syst. Biol.* 50, 913–925.
50. Caron, J.B., Conway Morris, S., and Shu, D. (2010). Tentaculate fossils from the Cambrian of Canada (British Columbia) and China (Yunnan) interpreted as primitive deuterostomes. *PLoS One* 5, e9586.
51. Holland, N.D., Holland, L.Z., and Holland, P.W.H. (2015). Scenarios for the making of vertebrates. *Nature* 520, 450–455.
52. He, K., Liu, J., Han, J., Ou, Q., Chen, A., Zhang, Z., Fu, D., Hua, H., Zhang, X., and Shu, D. (2023). Comment on “Ultrastructure reveals ancestral vertebrate pharyngeal skeleton in yunnanozoans”. *Science* 381, eade9707.
53. Patterson, C. (1988). Homology in classical and molecular biology. *Mol. Biol. Evol.* 5, 603–625.
54. Caron, J.B. (2005). *Banffia constricta*, a putative vetulicolid from the Middle Cambrian Burgess Shale. *Trans. R. Soc. Edinb. Earth Sci.* 96, 95–111.
55. Gillis, J.A., Fritzenwanker, J.H., and Lowe, C.J. (2012). A stem-deuterostome origin of the vertebrate pharyngeal transcriptional network. *Proc. Biol. Sci.* 279, 237–246.
56. Garstang, W. (1928). The morphology of the Tunicata, and its bearings on the phylogeny of the Chordata. *J. Cell Sci.* S2–72, 51–187.
57. Simakov, O., Kawashima, T., Marlétaz, F., Jenkins, J., Koyanagi, R., Mitros, T., Hisata, K., Bredeson, J., Shoguchi, E., Gyoja, F., et al. (2015). Hemichordate genomes and deuterostome origins. *Nature* 527, 459–465.
58. Kaplan, N., Razy-Krajka, F., and Christiaen, L. (2015). Regulation and evolution of cardiopharyngeal cell identity and behavior: insights from simple chordates. *Curr. Opin. Genet. Dev.* 32, 119–128.
59. Miyamoto, N., and Wada, H. (2013). Hemichordate neurulation and the origin of the neural tube. *Nat. Commun.* 4, 2713.
60. Rahman, I.A., Zamora, S., Falkingham, P.L., and Phillips, J.C. (2015). Cambrian cinctan echinoderms shed light on feeding in the ancestral deuterostome. *Proc. Biol. Sci.* 282, 20151964.
61. Pani, A.M., Mullarkey, E.E., Aronowicz, J., Assimacopoulos, S., Grove, E.A., and Lowe, C.J. (2012). Ancient deuterostome origins of vertebrate brain signalling centres. *Nature* 483, 289–294.
62. Budd, G.E., and Jensen, S. (2000). A critical reappraisal of the fossil record of the bilaterian phyla. *Biol. Rev.* 75, 253–295.
63. Lacalli, T.C. (2005). Protochordate body plan and the evolutionary role of larvae: old controversies resolved? *Can. J. Zool.* 83, 216–224.

64. Gee, H. (2018). Across the Bridge: Understanding the Origin of the Vertebrates (University of Chicago Press).
65. Deline, B., Greenwood, J.M., Clark, J.W., Puttick, M.N., Peterson, K.J., and Donoghue, P.C.J. (2018). Evolution of metazoan morphological disparity. *Proc. Natl. Acad. Sci. USA* **115**, E8909–E8918.
66. Bar-On, Y.M., Phillips, R., and Milo, R. (2018). The biomass distribution on Earth. *Proc. Natl. Acad. Sci. USA* **115**, 6506–6511.
67. Wright, A.M., and Hillis, D.M. (2014). Bayesian analysis using a simple likelihood model outperforms parsimony for estimation of phylogeny from discrete morphological data. *PLoS One* **9**, e109210.
68. Koch, N.M., and Parry, L.A. (2020). Death is on our side: paleontological data drastically modify phylogenetic hypotheses. *Syst. Biol.* **69**, 1052–1067.
69. Mongiardino Koch, N., Garwood, R.J., and Parry, L.A. (2021). Fossils improve phylogenetic analyses of morphological characters. *Proc. Biol. Sci.* **288**, 20210044.
70. Puttick, M.N., O'Reilly, J.E., Tanner, A.R., Fleming, J.F., Clark, J., Holloway, L., Lozano-Fernandez, J., Parry, L.A., Tarver, J.E., Pisani, D., and Donoghue, P.C.J. (2017). Uncertain-tree: discriminating among competing approaches to the phylogenetic analysis of phenotype data. *Proc. Biol. Sci.* **284**, 20162290.
71. Puttick, M.N., O'Reilly, J.E., Pisani, D., and Donoghue, P.C.J. (2019). Probabilistic methods outperform parsimony in the phylogenetic analysis of data simulated without a probabilistic model. *Palaeontology* **62**, 1–17.
72. Keating, J.N., Sansom, R.S., Sutton, M.D., Knight, C.G., and Garwood, R.J. (2020). Morphological phylogenetics evaluated using novel evolutionary simulations. *Syst. Biol.* **69**, 897–912.
73. Xie, W., Lewis, P.O., Fan, Y., Kuo, L., and Chen, M.H. (2011). Improving marginal likelihood estimation for Bayesian phylogenetic model selection. *Syst. Biol.* **60**, 150–160.
74. Kass, R.E., and Raftery, A.E. (1995). Bayes factors. *J. Am. Stat. Assoc.* **90**, 773.
75. Bergsten, J., Nilsson, A.N., and Ronquist, F. (2013). Bayesian tests of topology hypotheses with an example from diving beetles. *Syst. Biol.* **62**, 660–673.
76. Huelsenbeck, J.P., and Bollback, J.P. (2001). Empirical and hierarchical Bayesian estimation of ancestral states. *Syst. Biol.* **50**, 351–366.

## STAR★METHODS

### KEY RESOURCES TABLE

| REAGENT or RESOURCE   | SOURCE   | IDENTIFIER  |
|---|--|---|
| Deposited data  |  |   |
| Morphological character matrices in NEXUS format and as readable Mesquite files | This study   | Data S1, S2, and S3   |
| Software and algorithms   |  |   |
| MrBayes 3.2.6   | Ronquist et al. <sup>48</sup>  | <a href="http://nbisweden.github.io/MrBayes/">http://nbisweden.github.io/MrBayes/</a> |
| Other   |  |   |
| Pikaia specimens  | National Museum of Natural History, Smithsonian Institution; Royal Ontario Museum, Invertebrate Paleontology | USNM, ROMIP   |

### RESOURCE AVAILABILITY

#### Lead contact

Further information and requests should be directed to and will be fulfilled by the lead contact, Giovanni Mussini ([gm726@cam.ac.uk](mailto:gm726@cam.ac.uk)).

#### Materials availability

All specimens of *Pikaia* illustrated and analyzed in this study are deposited at the Royal Ontario Museum (ROMIP) or at the National Museum of Natural History, Smithsonian Institution (USNM), with accession numbers provided in the captions of Figures 1, 2, and S1. All data analyzed in this study are available as part of the Report, Figures 1, 2, 3, 4, and S1–S4, or in the Data S1.

#### Data and code availability

Our main phylogenetic dataset is available as a readable Mesquite file in Data S2, with character definitions listed in Data S1. Our alternative phylogenetic dataset is provided as a Mesquite file in Data S3. The parameters used for the phylogenetic analysis are described in the STAR Methods section below. Details of the MrBayes code used in our phylogenetic analyses are available in our Data S1.

### EXPERIMENTAL MODEL AND SUBJECT DETAILS

Photographs of previously described specimens of *Pikaia*<sup>3</sup> were made and provided by Jean-Bernard Caron. All illustrated specimens are deposited at the Royal Ontario Museum (ROM) or at the National Museum of Natural History, Smithsonian Institution (USNM). Accession numbers are provided in the captions of Figures 1, 2, 3, and S1.

### METHOD DETAILS

Phylogenetic analyses were performed using Bayesian Inference (BI), recently shown to be more robust to missing morphological data than alternative parsimony-based techniques<sup>67–70</sup> and generally outperform them in topological accuracy.<sup>70–72</sup> Markov chain Monte Carlo (MCMC) tree searches were performed in MrBayes 3.2.7<sup>48</sup> under a MK + gamma model.<sup>49</sup> Two parallel runs of 100,000,000 generations were requested, with 25% of samples discarded as burn-in. Our analyses only included characters which are parsimony informative ('informative' using the lset function) to account for the ascertainment bias. Convergence was checked using the sump command (standard deviation of split frequencies<0.01, ESS scores>200, PSRF~1.0 across all parameters) and the results visualized as a majority-rule consensus tree (Figure 4A). The MCMC search was repeated using alternative models, topological constraints, character coding, and taxon sampling (see Data S1 and S3).

To test the sensitivity of our topology, we reran our analyses using two datasets with alternative scorings of key characters (see Data S1 and S3 for alternative phylogenetic dataset). To estimate the marginal likelihood of our original tree (Figure 4A) against a scenario of vetulicolian monophly, the MCMC search was also repeated after constraining vetulicolians as a clade (Data S1; Figure S4A). Then, a stepping-stone sampling analysis<sup>73</sup> (SSA) was performed for both resulting topologies by applying hard constraints to all nodes and using two independent runs of sampling, with 40,000,000 generations (~10 times the highest number required for

convergence) requested. Both analyses used 50 steps. A Bayes factor comparison<sup>74</sup> was used to test support for the original and alternative, monophyletic topologies (Data S1). Bayes factors for hypothesis testing were interpreted after Bergsten et al.<sup>75</sup> (Table S1).

An ancestral states reconstruction (ASR) was performed on the unconstrained Bayesian tree (Figure 4A; Data S1) using the method outlined in Huelsenbeck and Bollback<sup>76</sup> to integrate phylogenetic uncertainty across all parameters, including topology. Hard constraints were applied across the entire tree, with model settings matching those of the MCMC search. Ancestral state probabilities were recovered using the report function and visualized through Tieplots (Figure 4A).